Contribution from the Anorganisch-Chemisches Institut der Universität Münster, Wilhelm-Klemm-Strasse 8, D-4400 Münster, Germany

Electronic Structure of $NbTe_{10}^{3-}$, a Tellurium Cluster with an Encapsulated Metal Atom

Wolfgang Tremel†

Received September 9, 1991

The recently synthesized $NbTe_{10}^{3-}$ cluster is unique in having a transition metal atom encapsulated in a cluster of main group atoms. The electronic structure of this unusual compound is analyzed with the aid of extended Hückel calculations. The tellurium cluster is stabilized by the interstitial because the large Te "bandwidth" and electronegativity match between Nb and Te allows Nb–Te bonding to relieve Te–Te antibonding interactions. The results of the calculations complement a localized bonding picture as suggested by Flomer and Kolis in the original paper. Two-electron oxidation of the $NbTe_{10}^{3-}$ species might be possible and would result in shorter bonds in the base of the Te_{10} birdcage.

Several decades ago, Zintl and co-workers described a considerable number of homopolyatomic anions of tin, lead, arsenic, antimony, bismuth, sulfur, selenium, and tellurium, which were formed by solution of the respective alkali metal alloys in ammonia.[1-3] The structural characterization of these so-called Zintl anions was precluded by the instability of the solid reaction products until Corbett and co-workers[4] provided a synthetic strategy for the stabilization of solid derivatives of many anions through complexation of the alkali metals with cryptands.[4,5] During the last decade, a wide variety of novel compounds was made.[4] More recently, compounds containing Zintl-type anions coordinated to transition metal atoms were reported, two striking examples being $[Tl_6Fe_{10}(CO)_{36}]^{6-}$ (**1**)[6] and $[Bi_4Fe_4(CO)_{13}]^{2-}$ (**2**).[7]

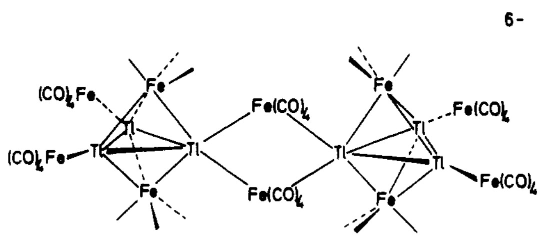

1

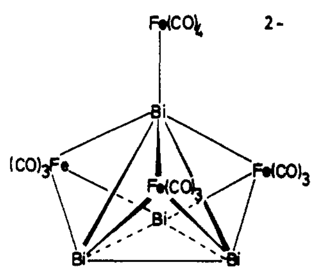

2

Other amazing hybrid clusters from main group elements and transition metal atoms are $^1_\infty[Rb(NbAs_8)]^{2-}$,[8] "inorganic" triple-decker compounds such as $Cp^*MoP_6MoCp^*$ made by Scherer and co-workers,[9] or the recently synthesized $[Sn_9Cr(CO)_3]^{4-}$ cluster.[10] The bonding in the last three cases can understood by applying the Zintl–Klemm–Busmann[11] or (appropriately modified[6,7,9]) Wade–Mingos[12] rules. For instance, the $(As^-)_8$ ligand in $^1_\infty[Rb(NbAs_8)]^{2-}$ is isoelectronic and isostructural with the S_8 molecule, and the structure of this polymeric dianion is easily rationalized as a quasi-one-dimensional stack of Rb^+ and Nb^{5+} cations and $(As^-)_8$ anions, which are separated by cation stacks in the solid-state structure. The bonding situation in **1** and **2** is more complex in that the usual electron-counting rules are either violated or not applicable. The unusual structure of **2** is based on a tetrahedral array of bismuth atoms capped on three faces by $Fe(CO)_3$ groups with one $Fe(CO)_4$ group attached to the unique bismuth atom. The resulting structure is related to that of cage compounds such as P_7^{3-},[13] As_7^{3-},[14] or Sb_7^{3-}.[15] Clearly, those

Table I. Parameters Used in Extended Hückel Calculations

orbital		H_{ii}, eV	ζ_1	ζ_2	$C_1{}^a$	$C_2{}^a$
S	3s	−20.00	1.82			
	3p	−13.30	1.82			
Te	5s	−20.80	2.51			
	5p	−14.80	2.16			
Nb	4d	−12.10	4.08	1.64	0.6401	0.5516
	5s	−10.10	1.89			
	5p	−6.86	1.85			

^{a} These are the coefficients in the double-ζ expansion.

† Current address: Institut für Anorganische und Analytische Chemie der Johannes Gutenberg-Universität Mainz, J.J.-Becherweg 24, D-6500 Mainz, Germany.

(1) Zintl, E.; Goubeau, J.; Dullenkopf, W. *Z. Phys. Chem., Abt. A* **1931**, *154*, 1.
(2) Zintl, E.; Harder, A. *Z. Phys. Chem., Abt. A* **1931**, *154*, 47.
(3) Zintl, E.; Dullenkopf, W. *Z. Phys. Chem., Abt. B* **1932**, *16*, 83.
(4) (a) Corbett, J. D. *Chem. Rev.* **1985**, *85*, 383. (b) Corbett, J. D.; Critchlow, S. C.; Burns, R. C. *ACS Symp. Ser.* **1983**, *232*, 95.
(5) Lehn, J. M. *Acc. Chem. Res.* **1978**, *11*, 49.
(6) Whitmire, K. H.; Ryan, R. R.; Wassermann, H. J.; Albright, T. A.; Kang, S.-K. *J. Am. Chem. Soc.* **1986**, *108*, 6831.
(7) Whitmire, K. H.; Churchill, M. R.; Fettinger, J. C. *J. Am. Chem. Soc.* **1985**, *107*, 1056. Whitmire, K. H.; Albright, T. A.; Kang, S.-K.; Churchill, M. R.; Fettinger, J. C. *Inorg. Chem.* **1986**, *25*, 2799.
(8) v. Schnering, H.-G.; Wolf, J.; Weber, D.; Ramirez, R.; Meyer, T. *Angew. Chem.* **1986**, *98*, 372; *Angew. Chem., Int. Ed. Engl.* **1986**, *25*, 353.
(9) (a) Scherer, O. J.; Sitzmann, H.; Wolmershäuser, G. *Angew. Chem.* **1985**, *97*, 358; *Angew. Chem., Int. Ed. Engl.* **1985**, *24*, 351. Related P_5 complexes have been reported as well: Scherer, O. J.; Schwall, J.; Wolmershäuser, G.; Kaim, W.; Gross, R. *Angew. Chem.* **1986**, *98*, 349; *Angew. Chem., Int. Ed. Engl.* **1986**, *25*, 363. For a review see: Scherer, O. J. *Comments Inorg. Chem.* **1987**, *6*, 1. (b) Theoretical analyses may be found in: Jemmis, E. D.; Reddy, A. C. *Organometallics* **1988**, *7*, 1561. Tremel, W.; Hoffmann, R.; Kertesz, M. *J. Am. Chem. Soc.* **1989**, *111*, 2030. Tremel, W.; Hoffmann, R.; Jemmis, E. D. *Inorg. Chem.* **1989**, *28*, 1213.
(10) Eichhorn, B. W.; Haushalter, R. C.; Pennington, W. T. *J. Am. Chem. Soc.* **1988**, *110*, 8704. The first spectroscopic evidence for a metalated Sn_9^{4-} cluster was reported by: Teixidor, F.; Luetkens, M. L.; Rudolph, R. W. *J. Am. Chem. Soc.* **1983**, *105*, 149.
(11) (a) Zintl, E.; Woltersdorf, G. *Z. Elektrochem. Angew. Phys. Chem.* **1935**, *41*, 876. Zintl, E. *Angew. Chem.* **1936**, *52*, 1. (b) Klemm, W.; Busmann, E. *Z. Anorg. Allg. Chem.* **1963**, *319*, 297. Klemm, W. *Proc. Chem. Soc. London* **1958**, 329. (c) Schäfer, H.; Eisenmann, B.; Müller, W. *Angew. Chem.* **1973**, *85*, 742; *Angew. Chem., Int. Ed. Engl.* **1973**, *12*, 694. Schäfer, H. *Annu. Rev. Mater. Sci.* **1985**, *15*, 1.
(12) (a) Mingos, D. M. P. *Acc. Chem. Res.* **1984**, *17*, 311. (b) Mingos, D. M. P. In *Comprehensive Organometallic Chemistry*; Wilkinson, G., Stone, F. G. A., Abel, E. W., Eds.; Pergamon Press: Oxford, U.K., 1981. (c) Mason, R.; Mingos, D. M. P. *MTP Int. Rev. Sci.: Phys. Chem., Ser. Two* **1975**, *11*, 121. (d) Wade, K. *Adv. Inorg. Chem. Radiochem.* **1976**, *18*, 1. (e) Wade, K. *Chem. Br.* **11**, 177. (f) Wade, K. *Inorg. Nucl. Chem. Lett.* **1972**, *8*, 559, 563. (g) Wade, K.; *J. Chem. Soc., Chem. Commun.* **1971**, 792. (h) Mingos, D. M. P. *Nature (London), Phys. Sci.* **1972**, *236*, 99. (i) Wade, K. *Electron Deficient Compounds*; Nelson: London, 1971.
(13) von Schnering, H.-G.; Dahlmann, W. *Naturwissenschaften* **1971**, *58*, 623.

0020-1669/92/1331-1030$03.00/0

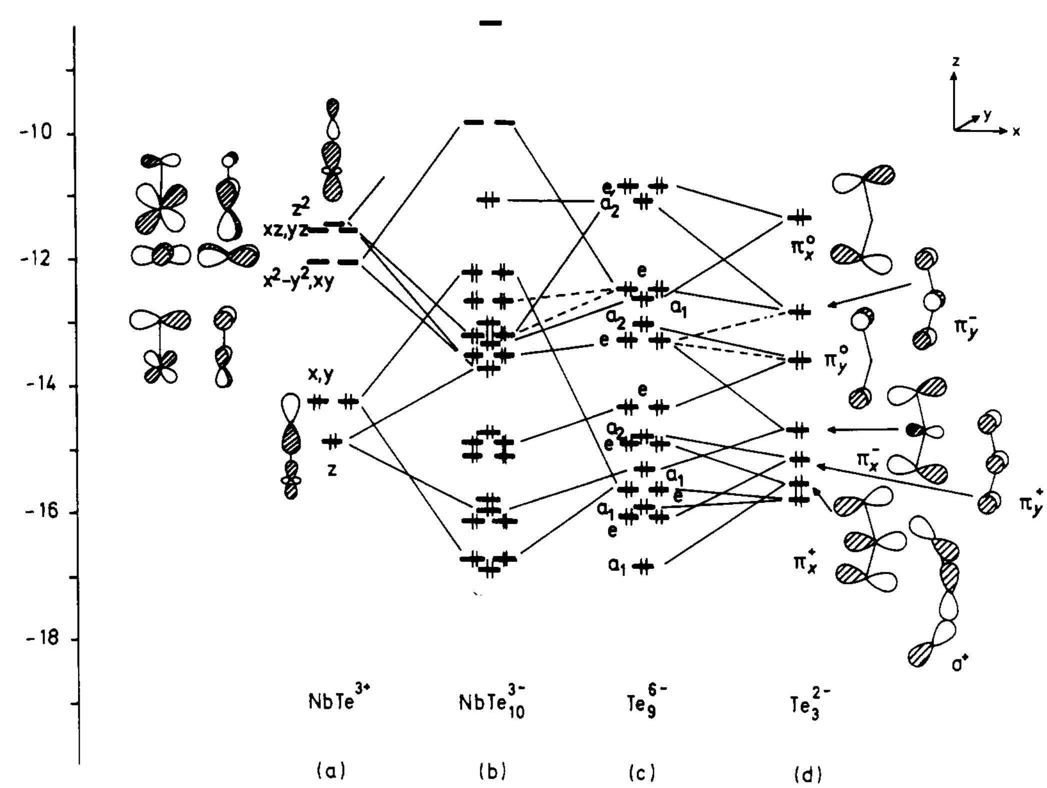

Figure 1. Interaction diagram for the frontier orbitals of $NbTe_{10}^{3-}$. On the right, three Te_3^{2-} groups (d) are combined with a Te_9^{6-} trimer (c). In the following step, this trimer is allowed to interact with $NbTe^{3+}$ (a) to form the $NbTe_{10}^{3-}$ anion (b).

species that violate the electron-counting rules attract attention by probing the limits of our chemical and theoretical understanding.

A unique molecular compound, $NbTe_{10}^{3-}$, a tellurium "cluster" containing an interstitial Nb atom was reported by Flomer and Kolis.[16] The anion, which is shown in two different perspectives in **3** and **4**, possesses idealized C_3 symmetry. The tellurium cage

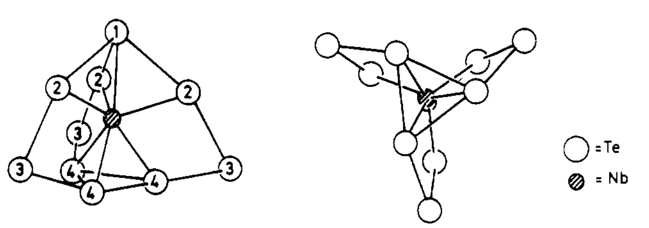

3 4

of this remarkable compound also bears similarity to the structure of Zintl anions such as Sb_7^{3-},[15] but now each of the vertical bonds is bridged by an additional Te atom. The Nb atom sits at the center of the cage, and it is coordinated by the atoms of the Sb_7^{3-}-like Te_7 fragment. The Te–Te distances within the cluster, which are in the range between 2.75 and 3.16 Å, display a considerable variation.[17] There are several ways of breaking the cluster into its constituents. One natural way of partitioning uses the hierarchy of bond distances. Following this line of thought, the $NbTe_{10}^{3-}$ cluster can be broken into three Te_3^{2-} [13] fragments, one apical Te^{2-} anion, and one Nb^{5+} cation. For the sake of simplicity, we will start in our analysis from an anion with idealized C_{3v} symmetry. In the final step of our discussion, this symmetry contraint will be lifted.

The orbitals of a triatomic Te_3^{2-} chain are easy to describe. There are four sets of orbitals, Te 5s, 5x, 5y, and 5z, which will combine in a fashion to give one bonding, one nonbonding, and one antibonding combination. The s orbitals and one linear combination of the p orbitals are involved in σ-type interactions, the remaining two sets of p orbitals give rise to π interactions. There will be some mixing between orbitals of same symmetry, but the general picture remains valid. For Te_3^{2-} the σ, π, and π^* orbitals are filled. As a result, we are left with a single bond between the Te atoms.

The interaction diagram in Figure 1 was constructed from an extended Hückel calculation[19] on $NbTe_{10}^{3-}$ in a C_{3v} symmetry. The energy levels of a Te_3^{2-} monomer are shown in Figure 1d; the corresponding orbitals are drawn out on the extreme right of the figure. Note the orbitals π_x^- and π_x^0 of the p_x set which have switched position with respect to the familiar ordering scheme. As can be seen from the figure, π_x^0 is pushed up by Te–Te antibonding 1,3 interactions in the bent Te_3^{2-} unit, while π_x^- is stabilized by Te–Te bonding 1,3 interactions.

Figure 1c shows the interaction of three Te_3^{2-} fragments in the absence of the central $NbTe^{3+}$ unit. For distances of 4.42 Å between the Te(2) atoms and 3.15 Å between the Te(4) atoms, we observe moderate level splittings. We do not draw out all the orbitals, but simply note that each set of trimer levels splits into an a and e set resembling the Walsh orbitals of cyclopropane.[20] Using the symmetry properties of the Te_9^{6-} fragment, it is easy to see that the radial orbitals transform as a_1 + e and the tangential ones as a_2 and e. For the radial orbitals, the splitting puts the totally bonding a_1 below e; a_2 is above e for the tangential ones.

(14) (a) Critchlow, S. C.; Corbett, J. D. *Inorg. Chem.* **1984**, *23*, 770. (b) Schmettow, W.; von Schnering, H.-G. *Angew. Chem., Int. Ed. Engl.* **1977**, *16*, 857.
(15) Adolphson, D. J.; Corbett, J. D.; Merryman, D. J. *J. Am. Chem. Soc.* **1976**, *98*, 7234.
(16) Flomer, W. A.; Kolis, J. W. *J. Am. Chem. Soc.* **1988**, *110*, 3682.
(17) Variable distances in this range are known from a number of solid-state and molecular compounds. For leading references see: Böttcher, P. *Angew. Chem.* **1988**, *100*, 781; *Angew. Chem., Int. Ed. Engl.* **1988**, *27*, 759. Bogan, L. E., Jr.; Rauchfuss, T. B.; Rheingold, A. L. *J. Am. Chem. Soc.* **1985**, *107*, 3843.
(18) Cisar, A.; Corbett, J. D. *Inorg. Chem.* **1977**, *16*, 632. Valentine, D. Y.; Cavin, O. B.; Yahel, H. L. *Acta Crystallogr., Sect. B* **1977**, *B33*, 1389. Böttcher, P.; Keller, R. *Z. Anorg. Allg. Chem.* **1986**, *542*, 144.
(19) (a) Hoffmann, R.; Lipscomb, W. N. *J. Chem. Phys.* **1962**, *36*, 2179, 3489; **1962**, *37*, 2872. (b) Hoffmann, R. *J. Chem. Phys.* **1963**, *39*, 1397. (c) Ammeter, J. H.; Bürgi, H.-B.; Thibeault, J. C.; Hoffmann, R. *J. Am. Chem. Soc.* **1978**, *100*, 3686.
(20) Walsh, A. D. *J. Chem. Soc.* **1953**, 2266.

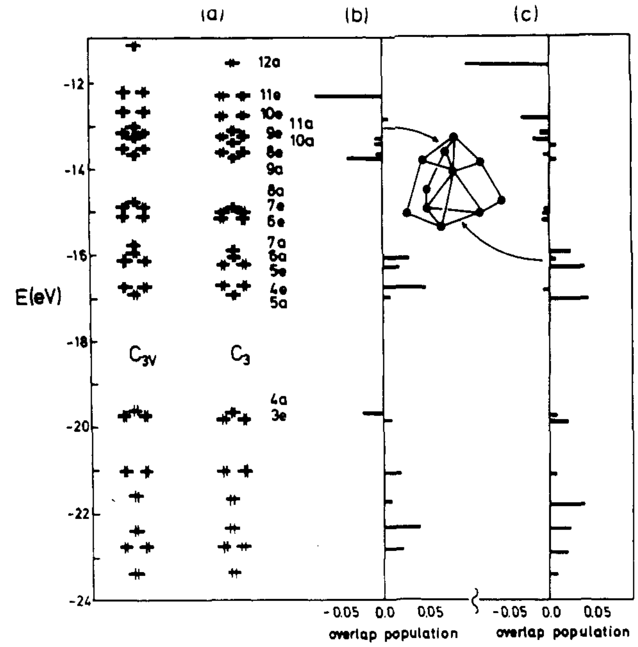

Figure 2. Energy levels of $NbTe_{10}^{3-}$ (a) and orbital contributions to the Te(1)–Te(2) (b) and Te(4)–Te(4) (c) overlap populations.

The reader is referred to several detailed discussions of the degenerate orbitals.[21]

The interactions of the orbitals can be qualitatively understood from the magnitudes of the level splittings. The radial combinations resulting from σ^+ split very little. Those resulting from combining π_x^+, π_x^-, and π_x^0 as well as the tangential combinations have larger interactions and split more. We note furthermore that, although the symmetry of the Te_9^{6-} unit is clearly C_{3v}, the orbitals can be classified as "symmetric" and "antisymmetric" with respect to a "horizontal mirror plane", π_x^+, π_y^+, π_x^-, and π_y^- being "symmetric" and σ^+, π_y^0, and π_x^0 being "antisymmetric". The same holds for their linear combinations. Similarly, the fragment orbitals of $NbTe^{3+}$ have a "nodal plane" passing through Nb. When both fragments are allowed to interact, strong interactions are expected between xz, yz on $NbTe^{3+}$ and their "antisymmetric" partners on the Te_9^{6-} fragment. Likewise, the second set of orbitals ($x^2 - y^2, xy$) and the a_1 orbitals of the central $NbTe^{3+}$ unit should strongly interact with their "symmetric" partners on the Te_9^{6-} fragment. For Te_9^{6-}, there is no net bonding between the Te_3^{2-} fragments.

Now we allow the $NbTe^{3+}$ unit and Te_9^{6-} trimer to interact. The energy levels of the $NbTe^{3+}$ fragment are shown in Figure 1a; its orbitals are drawn out on the extreme left of the figure. There are three relatively low-lying orbitals, z and $x + y$ (a_1 + e), centered on Te 5p. Next come Nb $x^2 - y^2$ and xy (e), which do not interact with the axial Te atom for symmetry reasons. Above them are Nb xz and yz (e) and z^2 (a_1), the antibonding counterparts of the low-lying z and x, y orbitals.

The a_2 orbitals derived from the tangential π_y^- orbitals of the Te_3^{2-} units do not find any symmetry match among the $NbTe^{3+}$ fragment orbitals and remain unchanged. They make up the HOMO of the $NbTe_{10}^{3-}$ anion. This level is severely destabilized by Te–Te repulsions of the Te_3^{2-} groups and is located just below the metal d block.

Several a_1 and e orbitals of the Te_9^{6-} fragment interact strongly with the corresponding symmetry combinations of the central $NbTe^{3+}$ unit. The most vital interactions are those between the empty xz, yz and filled symmetry partners on the Te_9^{6-} fragment. The interaction is large ($|\langle(xz, yz)|(Te_3^{2-})\rangle| = 0.27$), and the outcome is a stabilization by approximately 2 eV. Similarly, the "symmetric" $x^2 - y^2$, xy combination interacts strongly with the e sets descending from π_x^- and π_y^-. z^2 and z ($NbTe^{3+}$) interact in a typical three-orbital pattern with a_1 (π_x^-). These interactions basically take care of the Nb–Te bonds.

In addition, we observe strong mixing between *occupied* orbitals: the e combination derived from σ^+ has two large lobes directed toward the Te atom of the central Nb–Te unit. In fact, the repulsive effect dominates. At a Te–Te distance of 3.15 Å, the bonding combination is stabilized significantly, but the antibonding combination is pushed up by more than 3 eV. For an electron count corresponding to $NbTe_{10}^{3-}$, the anion comes out nicely as closed-shell diamagnetic species—in agreement with experiment.

Having understood the main interactions within the cage compounds, we approach the electronic structure of the real molecule by lifting the symmetry constraint that we imposed initially in order to simplify the analysis. As it turns out, not very much happens when the molecule is allowed to relax from C_{3v} to C_3 symmetry. The HOMO is stabilized by approximately 0.5 eV. A pictorial explanation can easily be given. Upon distortion, strongly antibonding interactions between the Te(4) atoms, which make up the bottom plane of the cluster, are relieved. A second-order mixing is effective, which mixes some contribution of **5**, a low-lying unoccupied orbital (the highest MO shown in Figure 1b), into the HOMO **6** in a bonding fashion. Both orbitals, **5** and

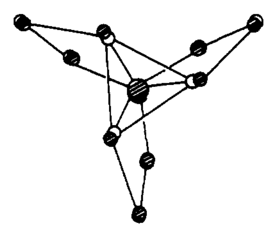

5

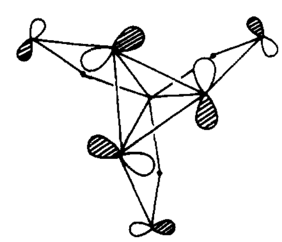

6

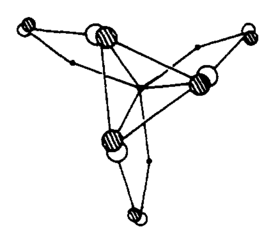

7

6, have different symmetries under C_{3v} but the same symmetries in the point group C_3. As a consequence of this mixing, the Te orbitals in **6**, which are strongly Te(4)–Te(4) antibonding, are slightly twisted out of the plane defined by the Te(4) atoms into more innocent regions of space in **7**. The net result is reduced Te–Te repulsion. This change manifests itself by an increase in the Te(4)–Te(4) overlap population from –0.022 to 0.014. This value for the reduced overlap population clearly establishes that there are in fact weak bonding Te–Te interactions all over the Te_{10} cage. While Te(4)–Te(4) repulsions are relieved, antibonding interactions are enhanced within the Te_3^{2-} fragments, resulting in a drop in the reduced overlap population from 0.470 to 0.439.

Figure 2 illustrates the bonding, nonbonding, and antibonding nature of the Te levels in the $NbTe_{10}^{3-}$ cluster. The figure is the cluster analogue of the COOP curve, which was initially created to describe the bonding in an extended three-dimensional solid.[22] The horizontal bars in Figure 2b,c represent the overlap populations from the levels in Figure 2a. Figure 2b shows the overlap populations between Te(1) and Te(2); Figure 2c, those between the Te(4) atoms. Bonding between Te(1) and Te(2) is significantly stronger than that between Te(4) atoms; less levels are antibonding

(21) (a) Albright, T. A.; Burdett, J. K.; Whangbo, M.-H. *Orbital Interactions in Chemistry*; Wiley-Interscience: New York, 1985. (b) Gimarc, B. M. *Molecular Structure and Bonding*; Academic Press: New York, 1979.

(22) (a) Hughbanks, T.; Hoffmann, R. *J. Am. Chem. Soc.* **1983**, *105*, 3528. (b) Wijeyesekera, S. D.; Hoffmann, R. *Organometallics* **1984**, *3*, 949. (c) Saillard, J.-Y.; Hoffmann, R. *J. Am. Chem. Soc.* **1984**, *106*, 2006. (d) An application for cluster compounds has been given in: Wheeler, R. A.; Hoffmann, R. *J. Am. Chem. Soc.* **1986**, *108*, 6605.

in Figure 2b, and their contributions to the overlap population are smaller. Most of the Te–Te bonding levels are located in the lower energy regime. Many features of Figure 2b,c are already visible in the interaction diagram in Figure 1 and have been discussed in the preceding text. The levels involved in Te(1)–Te(2) bonding between −17 and −10 eV are 4e, 6a, 9a, and 11e. The most significant Te(4)–Te(4) interactions are carried through 5a, 5e, 7a, and 12a. 4a and 6e had already been identified as the bonding combinations descending from σ^+ and x, y and from π_x^- and z, respectively; 11e is 4e's antibonding partner. 9a is the nonbonding orbital resulting from the three-level interaction of z, z^2, and π_x^-. 5a, which has not yet been mentioned, is the all-bonding combination of the π_x^+ orbitals. For Te(4)–Te(4) distances of 3.15 Å, a substantial stabilization results with respect to the levels of a single Te_3^{2-} fragment. 5e and 7a originate from π_y^+ and σ^+. These two moderately bonding orbitals are only slightly perturbed by the interaction of $NbTe^{3+}$ and Te_9^{6-}. Finally, 12a originates from the combination of π_y^-. It is strongly Te(2)–Te(2) antibonding and remains—as a consequence of its latent a_2 symmetry—unperturbed during the interaction of $NbTe^{3+}$ and Te_9^{6-}.

One important factor for the "cluster" stability is strong mixing between Nb and Te orbitals caused by the relatively small electronegativity differences[23] of Nb (1.8) and Te (2.1). In addition, the spread of the Te 5p orbital block is quite large, some 8–9 eV, pushing Te–Te antibonding states into the Nb d block. As a consequence, Te–Te antibonding interactions are "diluted", and—even though the Te 5p orbitals are formally filled—weak Te–Te bonding interactions remain.[24] Still, both the interaction diagram and the COOP curve show that the major portion of the Te 5p interactions are repulsive; most of the Te–Te bonding is carried through the Te 5s orbitals.

In their structural paper, Flomer and Kolis[16] describe the bonding within the cluster by assigning two-center–two-electron bonds to all "short" Nb–Te and Te–Te contacts and one/two lone pairs to the tri-/divalent Te atoms, respectively. This approach leaves four electrons to be distributed in one Te(1)–Te(2) and one Te(4)–Te(4) antibonding level. The Te(4)–Te(4) antibonding level finds a match in the HOMO of the $NbTe_{10}^{3-}$ cluster; a possible match for the Te(1)–Te(2) antibonding orbital may be found in the highest occupied degenerate level (labeled 11e in Figure 2).

Figures 1 and 2 show that one may expect a $NbTe_{10}^-$ mono- and a $NbTe_{10}^{2-}$ dianion to be stable. Computationally, a two-electron oxidation of the $NbTe_{10}^{3-}$ species leads to an increase of the Te(4)–Te(4) overlap population from 0.014 to 0.112. Since the HOMO of $NbTe_{10}^{3-}$ is centered almost exclusively on the Te(4) atoms, the remaining Nb–Te and Te–Te bonding is only marginally affected. For the oxidized species, our calculations prefer the C_{3v} geometry slightly over C_3. Reduction of the $NbTe_{10}^{3-}$ anion leads to a large increase in Te(4)–Te(4) repulsion; therefore, a reduced species is not expected to be stable.

Could we expect analogous compounds for the lighter chalcogens such as S or Se? To probe this question, calculations have been performed on a (hypothetical) NbS_{10}^{3-} species. Because the sulfur orbitals are much more contracted than those of Te,[25] the chalcogen "bandwidth" is quite narrow; i.e., the levels spread out over some 4 eV and are almost completely filled in the complex. Now the attractive forces between the main group atoms are lost, and severe S–S repulsions dominate. Although these results do not prove that NbS_{10}^{3-} does not exist, they do give evidence that attractive Te–Te interactions are important for the stabilization of the $NbTe_{10}^{3-}$ cluster.

Alternatively, one might envisage the possibility of using more electronegative metals than Nb as an electron sink to stabilize the cluster. However, besides the diffuseness of the S 3p compared to the Te 5p orbitals, the size of the central atom might be one other important factor for the cluster stability. The valence orbitals of a sufficiently electronegative transition metal would be too contracted to allow for seven chalcogen ligands in a capped trigonal prismatic geometry. Similarly, the size factor precludes the inclusion of transition metal atoms in related cagelike species such as As_7^{3-},[26a] Sb_7^{3-},[26b] or P_4S_3,[26c–e] leaving $NbTe_{10}^{3-}$ as a quite unique cluster compound.

Acknowledgment. This work was supported by the grant of a Liebig fellowship from the Verband der Chemischen Industrie to W.T. and by the Minister für Wissenschaft und Forschung des Landes Nordrhein-Westfalen through the Benningsen-Foerder program. The computing equipment was purchased through a grant from the Deutsche Forschungsgemeinschaft (DFG, Kr 406/9-1). Helfpul comments by a knowledgeable reviewer are gratefully acknowledged.

Appendix

All the calculations were performed by using the extended Hückel method[19a,b] with weighted H_{ij}'s.[19c] Experimental bond lengths were used for $NbTe_{10}^{3-}$. The values for the H_{ii}'s and the orbital exponents are listed in Table I.

Registry No. $NbTe_{10}^{3-}$, 114422-70-7.

(23) Pauling, L. *The Nature of the Chemical Bond*; Cornell University Press: Ithaca, NY, 1960.

(24) See for example the solid-state compounds $NbNiTe_5$ and $NbPdTe_5$: Liimatta, E. W.; Ibers, J. A. *J. Solid State Chem.* **1987**, *71*, 384; **1988**, *77*, 141. A theoretical analysis is given in: Halet, J.-F.; Hoffmann, R.; Tremel, W.; Liimatta, E. W.; Ibers, J. A. *Chem. Mater.* **1989**, *1*, 451.

(25) An intriguing fact is that many tellurium compounds exist, where Te occurs in the ionic limit as Te^{2-}. On the other hand, Te (and the other elements along the "Zintl line"—the diagonal of the periodic system) is observed in more "unusual" bonding situations. Two factors responsible for the anomalous behavior are the diffuse Te 5p orbitals and the inert electron pair effect, which is known for the post transition elements to contract the 5s orbital and to lower its energy. The global result for heavy main group elements is reduced lone pair repulsion.

(26) A number of structurally related cage molecules ligated to a transition metal atom have been reported. (a) $[As_7Cr(CO)_3]^{3-}$: Eichhorn, B. W.; Haushalter, R. C.; Huffman, J. C. *Angew. Chem.* **1989**, *101*, 1081; *Angew. Chem., Int. Ed. Engl.* **1989**, *28*, 1032. (b) $[Sb_7Mo(CO)_3]^{3-}$: Bolle, U.; Tremel, W. *J. Chem. Soc., Chem. Commun.*, submitted for publication. (c) $Mo(CO)_3(P_4S_3)$: Cordes, A. W.; Joyner, R. D.; Shores, R. D.; Dill, E. D. *Inorg. Chem.* **1974**, *13*, 132. (d) $[Ir(\mu\text{-}P_4S_3)Cl(CO)PPh_3]_2$: Ghilardi, C. A.; Midollini, S.; Orlandini, A. *Angew. Chem.* **1983**, *95*, 800; *Angew. Chem., Int. Ed. Engl.* **1983**, *22*, 790; *Angew. Chem. Suppl.* **1983**, 1066. (e) $[Pt(\mu_3\text{-}P_4S_3)(PPh_3)]_3$: DiVaira, M.; Peruzzini, M.; Stoppioni, P. *J. Chem. Soc., Dalton Trans.* **1985**, 291.